[30]B. T. Matthias, T. H. Geballe, K. Andres, E. Corenzwit, G. W. Hull, and J. P. Maita, Science 159, 530 (1968); T. H. Geballe, B. T. Matthias, K. Andres, J. P. Maita, A. S. Cooper, and E. Corenzwit, *ibid.* 160, 1443 (1968).

Localized Defects in PbTe[†]

Nelson J. Parada[*]

Materials Theory Group, Department of Electrical Engineering,
Massachusetts Institute of Technology, Cambridge, Massachusetts 02139
(Received 20 April 1970)

The electronic energy levels associated with vacancies in PbTe are obtained through the Green's-function method of Koster and Slater, the unperturbed Bloch functions being obtained from a relativistic $\vec{K} \cdot \vec{\pi}$ augmented-plane-wave (APW) energy-band calculation. APW one-electron energies were obtained at Γ and the corresponding eigenfunctions were used to obtain matrix elements of the relativistic momentum operator $\vec{\pi}$ between states at Γ. These energies and matrix elements were used in a $\vec{K} \cdot \vec{\pi}$ secular equation to obtain energies and wave functions at approximately 4300 points in the Brillouin zone. With 11 relativistic bands at Γ, excellent results were obtained. Localized Wannier functions were constructed by taking suitable linear combinations of the unperturbed Bloch functions and these Wannier functions provided the basis in which the energy levels in the presence of the perturbing impurity potential were found. We have solved the vacancy problem using Wannier functions from nine bands (five valence and four conduction) and 13 lattice sites. The results obtained from this calculation showed that Pb vacancies produce p-type PbTe, whereas Te vacancies produce n-type PbTe, and in both cases, carriers are present at all temperatures.

I. INTRODUCTION

It is our intention here to present a detailed account of the previously published calculation of the energy levels associated with vacancies in PbTe.[1] Lead telluride is known to have a NaCl crystal structure with a lattice constant of 6.452 Å (12.193 a.u.)[2] and to be a semiconductor with a direct gap of about 0.3 eV at room temperature.[3] The gap is located at the L point in the Brillouin zone. The measured and calculated electronic properties of the lead salts have been recently reviewed by Prakash,[4] in his work on the measurements of the optical-absorption edge of these salts and its variation with temperature and pressure. A very interesting property of the lead chalcogenide group of semiconductors is that they have ranges of non-stoichiometry, the lattice incorporating either excess lead or chalcogen with the corresponding defects. While excess lead produces a n-type semiconductor, excess chalcogen gives rise to a p-type material. Both cases are characterized by high mobilities at liquid-helium temperatures and it is not possible to freeze out the carriers at low temperatures.[5] It has been found that for excess chalcogen the principal defect is a singly ionized lead vacancy while for excess lead, the situation is not yet clear: For PbSe it seems that the principal defect is a doubly ionized intersticial Pb,[6,7] while for

PbS, a singly ionized sulfur vacancy appears to be the primary defect, although an appreciable concentration of doubly ionized intersticial Pb also exists.[8] On the other hand, a singly ionized tellurium vacancy is probably the most important defect in PbTe.[9] The theoretical study of vacancies in PbTe, therefore, presents the possibility of explaining the behavior described above.

The defect problem associated with a Pb and a Te vacancy is solved here in a manner similar to that used by Callaway and Hughes[10] for single and divacancies in silicon, that is, by applying the Green's-function method of Koster and Slater,[11] which has also been successfully used in the study of impurities in metals,[12] and in the problem connected with scattering of excitations in solids by localized imperfections.[13] The effect of the vacancy is treated as a time-independent localized potential and the perturbed wave functions are expanded in terms of Wannier functions of the unperturbed lattice. Because the latter functions are defined as linear combinations of Bloch functions, the knowledge of those wave functions, on a reasonable mesh of points in the Brillouin zone, is necessary.

The one-electron energy bands of PbTe were obtained by Conklin,[14] through a first-principles relativistic augmented-plane-wave (APW) calculation, and by Lin and Kleinman,[15] using a pseudopotential approach. Some experimental results can be very

well explained by Conklin's bands, and the effective masses[16] and deformation potentials[17] obtained with these bands are in good agreement with the experimental values. In principle, we can use the APW method to calculate the eigenfunctions and eigenvalues of the one-electron Hamiltonian at every point in the Brillouin zone. However for a low-symmetry point the calculation is prohibitive, due to the size of the secular equations to be diagonalized and to the computational time. What one does is to calculate the energy levels and the wave functions only for high-symmetry points and one or two points in the symmetry axes of the Brillouin zone. The energy bands are then sketched along these axes using the compatibility relations between the groups of the wave vector at these different points. In Sec. II we show how the eigenfunctions and the eigenvalues of the one-electron Hamiltonian can be obtained through a first-principles $\vec{K} \cdot \vec{\pi}$ interpolation scheme. In this method, if the energies, wave functions, and momentum matrix elements between these functions are known at a particular point in $\vec{k}$ space, $\vec{k}_0$ say, the energies and wave functions can be obtained at every other point. This method involves no approximation if all energy bands at $\vec{k}_0$ are included in the calculations. For a semiconductor, however, we are mainly interested in the conduction and valence bands, and we expect that bands with energy far away from these bands will give a small contribution in the calculations. Thus, if a reasonable number of bands around the conduction and valence bands is used in the $\vec{K} \cdot \vec{\pi}$ calculation, we expect good results near the Fermi level. The $\vec{K} \cdot \vec{\pi}$ method was first used by Cardona and Pollack[18] for germanium and silicon. The values for some of the energy gaps and momentum matrix elements were obtained from the experimental data on cyclotron resonance and optical measurements. The remaining parameters were assigned values suggested by the orthogonalized-plane-wave (OPW) calculation of Herman[19] and pseudopotential calculation of Brust[20] and were adjusted until the calculated energy bands agreed with the ultraviolet reflection data. Our calculation, however, differs from that of Cardona and Pollack in that in ours the relativistic bands at Γ and all momentum matrix elements between these bands were calculated. The information was used in a $\vec{K} \cdot \vec{\pi}$ secular matrix and the bands were obtained in a mesh of points in the Brillouin zone. The results were surprising; it was necessary to change only one of the nonrelativistic momentum matrix elements by 2.5% in order to fit the experimental gap, and at the points where Conklin performed his calculation, our results differ little from his. It is interesting to mention here that one of the main advantages of the $\vec{K} \cdot \vec{\pi}$ method is the saving of computation time. Once the single-group momentum matrix elements have

been calculated at $\vec{k}_0$, it takes less than 1 min on the IBM 360-MIT system, in order to obtain the energies and wave functions at a general point in the Brillouin zone, for a $\vec{K} \cdot \vec{\pi}$ secular matrix of dimension 30.

In Sec. III we solve the vacancy problem in PbTe, using the $\vec{K} \cdot \vec{\pi}$ APW bands. There we present the general theory of localized defects in semiconductors and the method of constructing vacancy potentials and Wannier functions. The theory is applied to PbTe and the above-mentioned behavior of this material can be well explained by the results obtained with nine $\vec{K} \cdot \vec{\pi}$ APW bands and 13 lattice sites.

II. $\vec{K} \cdot \vec{\pi}$ SCHEME

A. Theory

Let us consider the one-electron relativistic Hamiltonian derived from the Dirac equation by decoupling large and small components of the four-component wave function by means of sucessive applications of the Foldy-Wouthuysen unitary transformation.[21] In the absence of a magnetic field, and for coupling terms between the large and small components of the order of $(v/c)^5$, where v and c are, respectively, the velocities of the electron and of light, we obtain

$$H_0 = (2m)^{-1}\vec{p}^2 + V(\vec{r}) + (4m^2c^2)^{-1}[(\hbar\vec{\nabla}V\times\vec{p})\cdot\vec{\sigma}$$
$$+ 2^{-1}\hbar^2(\vec{\nabla}^2 V) - (2m)^{-1}\vec{p}^4] . \quad (2.1)$$

The first two terms are the kinetic and potential energies; the third is the spin-orbit coupling and the two last terms are the Darwin and mass-velocity corrections. The eigenfunctions of H_0 are Bloch functions $b_{n,i,\alpha}(\vec{k}, \vec{r})$ which transforms like the i partner of the double-group irreducible representation $\Gamma_\alpha^{(\vec{k})}$ of the group of the wave vector $\vec{k}$.

Suppose that at a particular point $\vec{k}_0$ in $\vec{k}$ space the Bloch functions $b_{n,i,\beta}(\vec{k}_0, \vec{r})$ and energy levels $E_n(\vec{k}_0)$ are known. We can then construct the Kohn-Luttinger functions

$$\chi_{n,i}(\vec{K}, \vec{r}) = b_{n,i,\beta}(\vec{k}_0, \vec{r})e^{i\vec{K}\cdot\vec{r}} , \quad (2.2)$$

where $\vec{K} = (\vec{k} - \vec{k}_0)$. These functions form a complete set of orthonormal functions and can be used as a basis for expanding a Bloch function at $\vec{k}$, i.e.,

$$b_{n,i,\gamma}(\vec{k}, \vec{r}) = \sum_{m'}\sum_j C_{n,i;m',j}$$
$$\times (\vec{K}) \chi_{m',j}(\vec{K}, \vec{r}). \quad (2.3)$$

Now, if Eq. (2.3) is substituted in Eq. (2.2) and the resulting equation is multiplied by $\chi_{n,i}(\vec{K}, \vec{r})^*$ and an integration over the whole crystal is performed, the following secular determinant is obtained for the expansion coefficients $C_{n,i;m',j}(\vec{K})$,

$$\det \left| [E_{m'}(\vec{k}_0) + (2m)^{-1}(\hbar\vec{K})^2 - (8m^3c^2)^{-1}(\hbar\vec{K})^4 \right.$$

$$\left. - E_n(\vec{k})]\delta_{n,m'}\delta_{i,j} + m^{-1}\hbar\vec{K}\cdot\vec{\pi}_{n,i;m',j}(\vec{K}) \right| = 0 ,$$

$$(2.4)$$

where

$$\vec{\pi}_{n,i;m',j}(\vec{K}) = \int d\vec{r}\, b_{n,i,\beta}(\vec{k}_0,\vec{r})^* \vec{\pi}\, b_{m',j,\beta'}(\vec{k}_0,\vec{r}),$$

$$(2.5)$$

$$\vec{\pi} = \vec{p} + (4mc^2)^{-1}(\hbar\vec{\sigma}\times\vec{\nabla}V) - (2m^2c^2)^{-1}$$

$$\times [\vec{p}^3 + (\hbar\vec{K})^2\vec{p} + 2^{-1}\hbar\vec{K}\vec{p}^2 + (\hbar\vec{K}\cdot\vec{p})\vec{p}] . \quad (2.6)$$

No approximation has been made until this point. However, the secular matrix (2.4) has infinite dimension and for practical purpose has to be truncated at some point. The dimensionality of the secular equation is choosen by considering the computational complexity vs the expected accuracy of the calculated energies and wave functions which depends not only on the number of bands used at $\vec{k}_0$, but also on the accuracy of the calculated energies and momentum matrix elements at this point.

Before we consider the practical application for PbTe, let us discuss more carefully the symmetry properties of the Bloch functions obtained through the $\vec{K}\cdot\vec{\pi}$ scheme. It can be shown[22] that for a general point $\vec{k}$

$$\{\alpha|\vec{t}_\alpha\}b_{n,i,\beta}(\vec{k},\vec{r}) = B(\alpha\vec{k},\vec{r})e^{i\gamma_\alpha(\vec{k})} , \quad (2.7)$$

where $\{\alpha|\vec{t}_\alpha\}$ is a space-group operation, $B(\alpha\vec{k},\vec{r})$ is a Bloch function with wave vector $\alpha\vec{k}$, and $\gamma_\alpha(\vec{k})$ is a real function of $\vec{k}$. But $\{\alpha|\vec{t}_\alpha\}$ being a space-group operation leaves the crystal lattice and the electron charge density unchanged. Then, $\{\alpha|\vec{t}_\alpha\}$ will interchange members of the star of $\vec{k}$. The phase factor $\exp\{i\gamma_\alpha(\vec{k})\}$ brought in by the symmetry operation $\{\alpha|\vec{t}_\alpha\}$ has to be specified and also one must express the function $B(\alpha\vec{k},\vec{r})$ on the right-hand side of Eq. (2.7) in terms of the functions in the star of $\vec{k}$. For a nondegenerate band it is reasonable to define $b_n(\vec{k},\alpha^{-1}\vec{r}) = b_n(\alpha\vec{k},\vec{r})$ and in this case

$$\{\alpha|\vec{t}_\alpha\}b_n(\vec{k},\vec{r}) = b_n(\alpha\vec{k},\vec{r})e^{i\alpha\vec{k}\cdot\vec{t}_\alpha} . \quad (2.8)$$

Recently, however, Callaway and Hughes[10] showed that if only nondegenerate bands are considered, it is necessary to define

$$\{\alpha|\vec{t}_\alpha\}b_n(\vec{k},\vec{r}) = \chi^{\Gamma\beta}(\alpha)e^{i\alpha\vec{k}\cdot\vec{t}_\alpha}b_n(\alpha\vec{k},\vec{r}) \quad (2.9)$$

in order that the periodic part of the Bloch function associated with band n vary smoothly in $\vec{k}$ space. In Eq. (2.9) $\chi^{\Gamma\beta}(\alpha)$ is the character of one of the one-dimensional representations Γ_β of the point group and can only have the values ± 1. This point is important in all problems where localized Wan-

nier functions have to be defined. Later Callaway[23] showed that Eq. (2.9) is a consequence of the $\vec{K}\cdot\vec{p}$ perturbation theory near $\vec{k}=0$ for a nondegenerate band. If Eq. (2.9) is satisfied at $\vec{k}=0$ it will be satisfied for all $\vec{k}$ for which the perturbation series converges. In this case $\chi^{\Gamma\beta}(\alpha)$ is the character of the irreducible representation of the band at $\vec{k}=0$. In Appendix A we determine the properties of the Bloch functions obtained in the $\vec{K}\cdot\vec{\pi}$ scheme in the case where the group of $\vec{k}_0$ is the point group of the crystal. We obtain that

$$\{\alpha|\vec{t}_\alpha\}b_{n,i,\beta}(\vec{k},\vec{r}) = e^{i\alpha\vec{k}\cdot\vec{t}_\alpha}b_{n,i,\beta}(\alpha\vec{k},\vec{r}) , \quad (2.10)$$

which shows that the application of one operation of the space group to a Bloch function at $\vec{k}$ will produce a Bloch function in the star, corresponding to the same band and partner as the original Bloch function at $\vec{k}$. The $\vec{K}\cdot\vec{\pi}$ method, however, does not produce Bloch functions whose periodic parts vary smoothly in the Brillouin zone. We can easily verify this by considering, for example, the region near $\vec{k}_0$. Consider a point $\vec{k}$ and a band n and assume that at $\vec{k}_0$ the i partner of this band corresponds to the i' partner of band n', i.e., $C_{n,i;m,j}(\vec{0}) = \delta_{m,n'}\delta_{j,i'}$. If we are seeking for a smooth function, then the last relation must hold approximately at every point $\vec{k}$ near $\vec{k}_0$. Consider now the Bloch function at $\alpha\vec{k}$. According to Eq. (A5),

$$C_{n,i;m,j}(\alpha\vec{k}) = \sum_l C_{n,i;m,l}(\vec{k})\Gamma_\beta^{(\vec{k}_0)}(\alpha)_{j,l}$$

$$\simeq C_{n,i;m,i'}(\vec{k})\Gamma_\beta^{(\vec{k}_0)}(\alpha)_{j,i'}\delta_{m,n'} ,$$

which shows us that the periodic part of the Bloch function will not vary smoothly near $\vec{k}_0$. For the purpose of obtaining localized Wannier functions we are interested in generating Bloch functions that exhibit reasonable continuity near $\vec{k}_0$. One way of doing this is to consider, for every α, a new set of values for the $\vec{K}\cdot\vec{\pi}$ expansion coefficients, which we will call $C'_{n,i;n',j}(\alpha\vec{k})$ such that they vary smoothly near $\vec{k}_0$. Define

$$C'_{n,i;n',j}(\alpha\vec{k}) = \sum_q \{[\Gamma_\beta^{(\vec{k}_0)}(\alpha)]^{-1}\}_{j,q} C_{n,i;n',q}(\alpha\vec{k}) .$$

$$(2.11)$$

In this case

$$C'_{n,i;n',j}(\alpha\vec{k}) = C_{n,i;n',j}(\vec{k}) . \quad (2.12)$$

The transformation we have performed is unitary, because the matrices for the representation at $\vec{k}_0$ are unitary. If bands n and n' are one dimensional, then

$$C'_{n,1;n',1}(\alpha\vec{k}) = \chi^{\Gamma\beta(\vec{k}_0)}(\alpha)C_{n,1;n',1}(\alpha\vec{k}) \quad (2.13)$$

which is similar to the result obtained by Callaway.[23] When $\vec{K}$ is large, probably other bands besides n' contribute significantly to band n at $\vec{k}$. In this case

the coefficients corresponding to these bands will not be continuous with the above transformation. Further considerations about the proper choice of the phases of Bloch functions will be made in Sec. III in connection with the study of Wannier functions in PbTe.

Now, if $\vec{k}$ is a symmetry point, i.e., there exist operations α other than identity such that $\alpha\vec{k}=\vec{k}$, Bloch functions at this point have to transform under α-like partners of the irreducible representations of the group of $\vec{k}$. In this case, by means of suitable rotations of the basis functions, the $\vec{K}\cdot\vec{\pi}$ matrix can be factored, each block corresponding to a certain irreducible representations of the group of $\vec{k}$. Only partners of the irreducible representations of the group of $\vec{k}_0$ compatible with partners of a certain irreducible representation of the group of $\vec{k}$ will enter the block corresponding to the latter representation.

B. Application to PbTe

Let us now apply the preceding theory to PbTe. Point $\vec{k}_0$ is chosen to be the Γ point in $\vec{k}$ space and in this case the group of $\vec{k}_0$ is the point group of the crystal. The Bloch functions and energy eigenvalues at $\vec{k}_0$ are obtained through an APW energy-band calculation.

Figure 1 shows schematically the nonrelativistic and full relativistic bands obtained at Γ through the APW calculation. In this figure and in the subsequent considerations we will represent the energy bands by the corresponding irreducible representations. Because this labeling is not unique, an extra index m is introduced. Thus ${}^{m}\Gamma_{n,i}$ will represent the i partner of the mth band that transforms like the irreducible representation Γ_n.
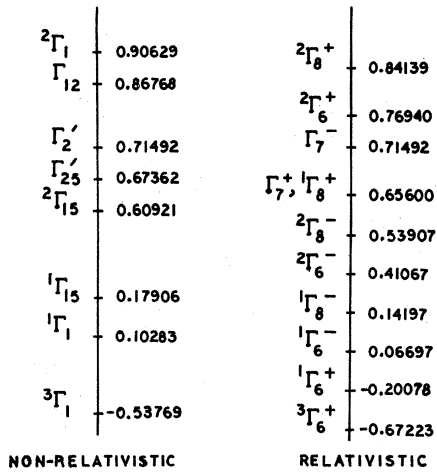
The transformation properties of the partners of

TABLE I. Transformation properties of the single-group irreducible representations at Γ.

Representation	Transformation properties
Γ_1	s
$\Gamma_{15,1}$	x
$\Gamma_{15,2}$	y
$\Gamma_{15,3}$	z
$\Gamma_{12,1}$	$(3)^{1/2}(x^2-y^2)$
$\Gamma_{12,2}$	$3z^2-r^2$
Γ_2'	xyz
$\Gamma_{25,1}'$	yz
$\Gamma_{25,2}'$	xz
$\Gamma_{25,3}'$	xy

the single-group irreducible representations are shown in Table I, where a system of coordinates with axes in the [100], [010], and [001] directions is considered. Table II shows how to write the partners of the double-group irreducible representations in terms of the single-group irreducible representations. In that table, $\Gamma_{n,i}(\Gamma_m)$ represents the i partner of the Γ_n double-group irreducible representation coming from the Γ_m single-group irreducible representation at Γ, and S_α and S_β are the common "spin-up" and "spin-down" functions. It can be observed that the partners of the double-group representations form Kramers pairs, i.e.,

TABLE II. Relations between partners of the double-group and single-group irreducible representations at Γ.

$$\Gamma_{6,1}^+(\Gamma_1) = \Gamma_1 S_\alpha$$

$$\Gamma_{6,2}^+(\Gamma_1) = \Gamma_1 S_\beta$$

$$\Gamma_{7,1}^+(\Gamma_{25}') = (3)^{-1/2}[(-i\Gamma_{25,1}'+\Gamma_{25,2}')S_\beta - i\Gamma_{25,3}'S_\alpha]$$

$$\Gamma_{7,2}^+(\Gamma_{25}') = (3)^{-1/2}[(-i\Gamma_{25,1}'-\Gamma_{25,2}')S_\alpha + i\Gamma_{25,3}'S_\beta]$$

$$\Gamma_{8,1}^+(\Gamma_{25}') = (6)^{-1/2}[(i\Gamma_{25,1}'+\Gamma_{25,2}')S_\alpha + 2i\Gamma_{25,3}'S_\beta]$$

$$\Gamma_{8,4}^+(\Gamma_{25}') = (6)^{-1/2}[(-i\Gamma_{25,1}'+\Gamma_{25,2}')S_\beta + 2i\Gamma_{25,3}'S_\alpha]$$

$$\Gamma_{8,3}^+(\Gamma_{25}') = (2)^{-1/2}(i\Gamma_{25,1}'-\Gamma_{25,2}')S_\alpha$$

$$\Gamma_{8,2}^+(\Gamma_{25}') = (2)^{-1/2}(i\Gamma_{25,1}'-\Gamma_{25,2}')S_\beta$$

$$\Gamma_{6,1}^-(\Gamma_{15}) = (3)^{-1/2}[(-i\Gamma_{15,1}+\Gamma_{15,2})S_\beta - i\Gamma_{15,3}S_\alpha]$$

$$\Gamma_{6,2}^-(\Gamma_{15}) = (3)^{-1/2}[(-i\Gamma_{15,1}-\Gamma_{15,2})S_\alpha + i\Gamma_{15,3}S_\beta]$$

$$\Gamma_{7,1}^-(\Gamma_2') = \Gamma_2' S_\alpha$$

$$\Gamma_{7,2}^-(\Gamma_2') = \Gamma_2' S_\beta$$

$$\Gamma_{8,1}^-(\Gamma_{15}) = (2)^{-1/2}(-i\Gamma_{15,1}+\Gamma_{15,2})S_\alpha$$

$$\Gamma_{8,4}^-(\Gamma_{15}) = (2)^{-1/2}(i\Gamma_{15,1}+\Gamma_{15,2})S_\beta$$

$$\Gamma_{8,3}^-(\Gamma_{15}) = (6)^{-1/2}[(\Gamma_{15,1}+\Gamma_{15,2})S_\alpha + 2i\Gamma_{15,3}S_\beta]$$

$$\Gamma_{8,2}^-(\Gamma_{15}) = (6)^{-1/2}[(-i\Gamma_{15,1}+\Gamma_{15,2})S_\beta + 2i\Gamma_{15,3}S_\alpha]$$

NON-RELATIVISTIC		RELATIVISTIC	
${}^2\Gamma_1$	0.90629	${}^2\Gamma_8^+$	0.84139
Γ_{12}	0.86768		
		${}^2\Gamma_6^+$	0.76940
Γ_2'	0.71492	Γ_7^+	0.71492
Γ_{25}'	0.67362	$\Gamma_7^+, {}^1\Gamma_8^+$	0.65600
${}^2\Gamma_{15}$	0.60921		
		${}^2\Gamma_8^+$	0.53907
		${}^2\Gamma_6^+$	0.41067
${}^1\Gamma_{15}$	0.17906	${}^1\Gamma_8^-$	0.14197
${}^1\Gamma_1$	0.10283	${}^1\Gamma_6^-$	0.06697
		${}^1\Gamma_6^+$	-0.20078
${}^3\Gamma_1$	-0.53769	${}^3\Gamma_6^+$	-0.67223

FIG. 1. Schematic representation of the energy levels at Γ for PbTe.

$\Gamma_{n,2} = \kappa T_{n,1}$, where κ is the time-reversal operator and for four-dimensional representations, $\Gamma_{n,4} = \kappa T_{n,1}$ and $\Gamma_{n,2} = \kappa T_{n,3}$.

In order to obtain the $\vec{K} \cdot \vec{\pi}$ secular matrix elements it is necessary to calculate the matrix elements of $\vec{\pi}$ between Bloch functions at Γ. The calculation of the matrix elements between the nonrelativistic bands of the first three terms in Eq. (2.6), which are $\vec{K}$ independent, was performed for PbTe. As it happens at the L point[16] the second and third terms give matrix elements which are 10^{-3} to 10^{-6} smaller than the corresponding momentum matrix elements and can be disregarded. The three other terms in Eq. (2.6), which are $\vec{K}$ dependent, and do not enter the effective-mass calculations, where $\vec{K}$ is assumed small, were studied. Results at Γ showed that they are also of the order of 10^{-3} to 10^{-6} compared with any other term, if $\vec{K}$ is limited to the first Brillouin zone. These considerations show us that only the momentum matrix elements themselves are important in the calculations. This does not mean that we are disregarding the relativistic corrections. What have been disregarded are the contributions of these terms to the $\vec{\pi}$ operator. Observe that the bands at Γ contain all relativistic corrections. Table III shows the momentum matrix elements between single-group representations at Γ which are different from zero by symmetry considerations. This can be obtained by noting that $\vec{p}$ transforms like Γ_{15} and using the transformation properties of Table II. The nonzero momentum matrix elements between double-group representations can be obtained through Tables II and III, and observing that for each Kramers pair,

$$\langle \Gamma_{n,i} | \vec{p} | \Gamma_{m,i} \rangle = \langle \Gamma_{n,j} | \vec{p} | \Gamma_{m,j} \rangle^*$$

and

$$\langle \Gamma_{n,i} | \vec{p} | \Gamma_{m,j} \rangle = -\langle \Gamma_{n,j} | \vec{p} | \Gamma_{m,i} \rangle^* .$$

The 11 independent momentum matrix elements were calculated using Conklin's nonrelativistic bands at Γ. Although a good energy convergence on the number of symmetrized APW (SAPW) was

obtained, the same was not true for all momentum matrix elements. A new APW band calculation was then performed with 15 SAPW's for each level. Although the energy levels and the mixing changed very little, an excellent convergence was now obtained for all momentum matrix elements. The new values, showed in Table IV, were then used in the $\vec{K} \cdot \vec{\pi}$ secular matrix which was diagonalized for values of $\vec{k}$ along the symmetry axes. The energy gap at L was found to be equal to 0.0256 Ry (0.340 eV) which is bigger than the experimental gap. A quantitative study of the influence of the various momentum matrix elements in the $\vec{K} \cdot \vec{\pi}$ bands, along the symmetry axes, was then performed. There are several elements whose variation changes the gap at L. However, there is one momentum matrix element, namely, $M_{1,2;15,2}$, which, while strongly changing the gap, also changes the bands at other symmetry points in such a way that the $\vec{K} \cdot \vec{\pi}$ bands move towards the Conklin's bands. The variation of the gap with $M_{1,2;15,2}$ is shown in Fig. 2. Owing to the symmetries in a fcc unit cell, energies and wave functions need to be calculated only for points

TABLE IV. Matrix elements of $(\hbar/m)\vec{p}$ between basis functions at Γ.

Matrix element	Value (a.u.)
$(\hbar/m)\ M_{1,1;15,1}$	0.969
$(\hbar/m)\ M_{1,1;15,2}$	0.250
$(\hbar/m)\ M_{1,2;15,1}$	−0.155
$(\hbar/m)\ M_{1,2;15,2}$	1.180
$(\hbar/m)\ M_{1,3;15,1}$	0.437
$(\hbar/m)\ M_{1,3;15,2}$	−0.225
$(6^{1/2}\hbar/2m)\ M_{12,1;15,1}$	0.534
$(6^{1/2}\hbar/2m)\ M_{12,1;15,2}$	−1.456
$(\hbar/m)\ M_{25,1;2,1}$	0.949
$(3^{1/2}\hbar/2m)\ M_{25,1;15,1}$	1.068
$(3^{1/2}\hbar/2m)\ M_{25,1;15,2}$	0.460

TABLE III. Nonzero momentum matrix elements between single-group irreducible representations at Γ.

$$M_{1,a;15,b} = \langle {}^a T_1 | p_x | {}^b T_{15,1} \rangle = \langle {}^a T_1 | p_y | {}^b T_{15,2} \rangle = \langle {}^a T_1 | p_z | {}^b T_{15,3} \rangle$$

$$M_{12,a;15,b} = \langle {}^a T_{12,1} | p_z | {}^b T_{15,1} \rangle = -\langle {}^a T_{12,1} | p_y | {}^b T_{15,2} \rangle$$

$$= -(3)^{1/2} \langle {}^a T_{12,2} | p_x | {}^b T_{15,1} \rangle = -(3)^{1/2} \langle {}^a T_{12,2} | p_y | {}^b T_{15,2} \rangle$$

$$= (3^{1/2}/2) \langle {}^a T_{12,2} | p_z | {}^b T_{15,3} \rangle$$

$$M_{25,a;2,b} = \langle {}^a T'_{25,1} | p_x | {}^b T'_2 \rangle = \langle {}^a T'_{25,2} | p_y | {}^b T'_2 \rangle = \langle {}^a T'_{25,3} | p_z | {}^b T'_2 \rangle$$

$$M_{25,a;15,b} = \langle {}^a T'_{25,1} | p_y | {}^b T_{15,3} \rangle = \langle {}^a T'_{25,1} | p_z | {}^b T_{15,2} \rangle$$

$$= \langle {}^a T'_{25,2} | p_z | {}^b T_{15,1} \rangle = \langle {}^a T'_{25,2} | p_x | {}^b T_{15,3} \rangle$$

$$= \langle {}^a T'_{25,3} | p_y | {}^b T_{15,1} \rangle = \langle {}^a T'_{25,3} | p_x | {}^b T_{15,2} \rangle$$
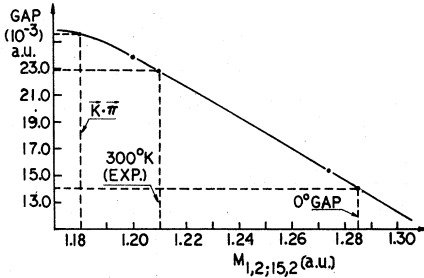
FIG. 2. Variation of the energy gap at L as a function of $M_{1,2;15,2}$.

in a region A corresponding to $\frac{1}{48}$ of the first Brillouin zone. A possible choice is $k_x \geqslant k_y \geqslant k_z$, $k_x \leqslant (2\pi/a)$ and $(k_x + k_y + k_z) \leqslant (3\pi/a)$. We have used a regular mesh of 152 points in A, the distance between two adjacents points in the mesh being $\Delta k_i = 0.20(\pi/a)$. This corresponds to 4288 points in the first Brillouin zone and is very suitable for interpolations of both the energy levels and the $\vec{K}\cdot\vec{\pi}$ coefficients of the wave functions. Figure 3 shows the $\vec{K}\cdot\vec{\pi}$ bands obtained in the symmetry axes. The circles in those figures represent the values obtained by Conklin's APW calculation. The general behavior of the bands in any other direction in $\vec{k}$ space is similar, with the exception that the band crossings occurring in the [100] axis are not allowed at general points.

Knowledge of the wave functions allows us to obtain the matrix elements of the linear momentum between the relativistic bands over the entire Brillouin zone. They were calculated on the 152 point regular mesh and the results used to calculate the optical dielectric constant $\epsilon(\vec{q}=0, \omega)$ of PbTe.[24] The comparison with the measured value of Cardona and Greenaway[25] for the real part of the dielectric constant showed that the calculated value agrees very well with the experiment.

III. LOCALIZED DEFECTS IN THE $\vec{K}\cdot\vec{\pi}$ APW SCHEME

A. General Theory

Let us assume that the perturbed crystal potential can be written as the sum of the unperturbed potential plus a time-independent term $U(\vec{r})$, that represents the effect of the imperfections. One seeks then for the solution of the stationary Schrödinger equation

$$[H_0 + U(\vec{r})]\,\Psi(\vec{r}) = E\,\Psi(\vec{r}) , \qquad (3.1)$$

where H_0 is the unperturbed one-electron Hamiltonian. In the Koster-Slater scheme,[11] the Wannier functions are used as the basis for the expansion of $\Psi(\vec{r})$ and the following secular matrix for the
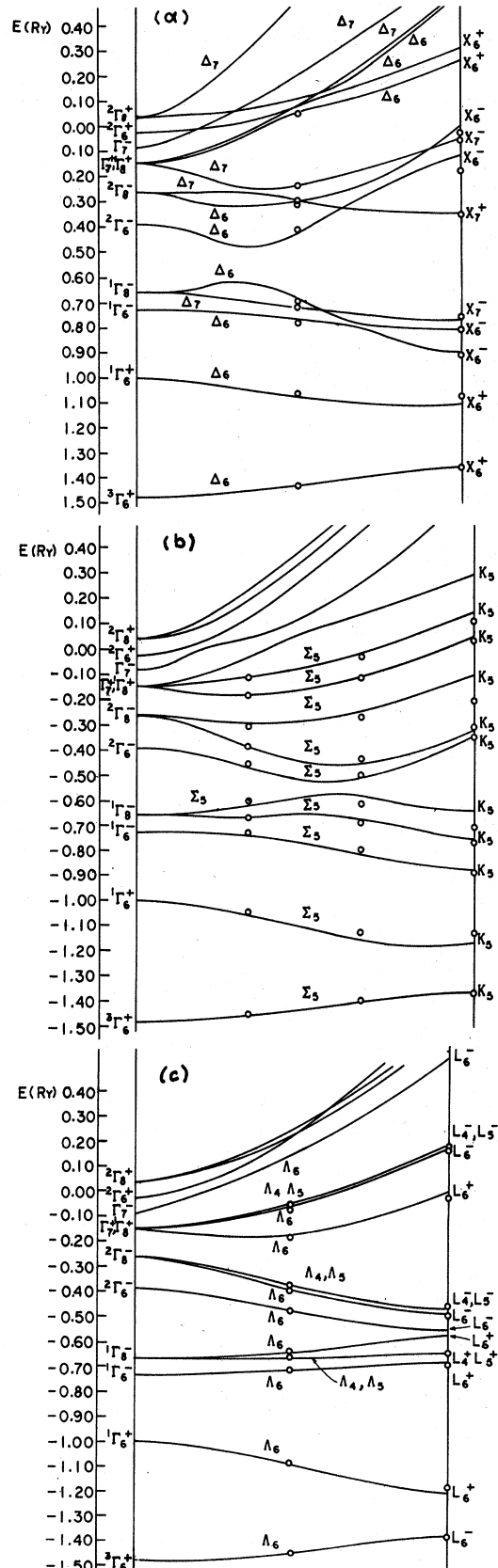

FIG. 3. $\vec{K}\cdot\vec{\pi}$ energy bands for the (a) [100] direction, (b) [110] direction, (c) [111] direction.

coefficients of expansion is obtained:

$$\det|\ I - GU\ | = 0 \ , \qquad (3.2)$$

where I is the identity matrix

$$G_{n',i';n,i}(\vec{R}_p - \vec{R}_{q'},\ E)$$

$$= N_{\vec{k}}^{-1}\sum_{\vec{k}}\delta_{n',n}\delta_{i',i}\,[E - E_n(\vec{k})]^{-1}e^{i\vec{k}\cdot(\vec{R}_p - \vec{R}_{q'})} \qquad (3.3)$$

is the general element of matrix G, with $N_{\vec{k}}$ being the number of allowed $\vec{k}$ vectors in the Brillouin zone,

$$U_{n',i';n,i}(\vec{R}_{q'},\ \vec{R}_q)$$

$$= \langle a_{n',i'}(\vec{r} - \vec{R}_{q'})|\ U(\vec{r})|\ a_{n,i}(\vec{r} - \vec{R}_q)\rangle \qquad (3.4)$$

is the general element of matrix U and

$$a_{n,i}(\vec{r} - \vec{R}_q) = \Omega_{\vec{k}}^{1/2}\int_{BZ}d\vec{k}\,b_{n,i,\beta}(\vec{k},\ \vec{r})e^{-i\vec{k}\cdot\vec{R}_q}e^{i\Theta_n(\vec{k})}$$

$$(3.5)$$

is the Wannier function for band n, partner i, and lattice site $\vec{R}_q$. $\Omega_{\vec{k}}$ is the volume of the first Brillouin zone and $\Theta_n(\vec{k})$ is a phase factor. These phase factors are necessary because if they are chosen properly, localized Wannier functions are obtained. The secular matrix in Eq. (3.2) has a general row or column characterized by the band index n, the partner index i, and the lattice site $\vec{R}_q$.

If the perturbation $U(\vec{r})$ and the Wannier functions are well localized, the matrix U can be well approximated as having only a finite number of non-zero elements which can be rearranged to appear in the upper-left corner of the matrix. Let us denote this part by U_{NN}. Then Eq. (3.2) can be written as

$$\det|\ I_{NN} - G_{NN}U_{NN}\ | = 0 \ , \qquad (3.6)$$

where G_{NN} and I_{NN} are, respectively, the block of the matrices G and I which correspond to the block U_{NN} of U_N. Equation (3.6) can be written as

$$\det|\ G_{NN}^{-1} - U_{NN}\ | = 0 \ , \qquad (3.7)$$

where G_{NN}^{-1} is the inverse of G_{NN}. Equation (3.7) is preferred over Eq. (3.6) because $I_{NN} - G_{NN}U_{NN}$ is not Hermitian, even though G_{NN} and U_{NN} are Hermitian. Energy E in Eq. (3.3) is a real number if we

are limited to states lying in the energy gap of the host material (bound states). In the case where we are dealing with states whose energies coincide with energies in the spectrum of H_0, as in the scattering problem, E must be allowed to have an infinitesimal imaginary part.

The definition (3.5) for the Wannier functions may present difficulties when the band structure of the material presents symmetry, accidental or quasi-degeneracies. Near quasidegeneracies, two different points of view can be taken when defining Wannier functions. According to the first point of view, the bands are not allowed to cross and are defined in their order of increasing energy. In this case a continuous energy band will be produced and the G matrix will have the proper asymptotic behavior for large values of E. The wave functions, however, may vary wildly in the zone, making the definition of localized Wannier functions more difficult, but not impossible. In this case, under the operations of the crystal point group, the localized Wannier functions may not exhibit simple transformation properties and large matrices may have to be diagonalized in solving the defect problem. The second point of view consists of departing from the above band ordering according to increasing energy by defining bands with Bloch functions whose periodic part varies slowly in $\vec{k}$ space. In this case the points where the quasidegeneracies occur have to be excluded from the definition of the Wannier functions and consequently the G matrix does not have the proper behavior for large values of E. But localized Wannier functions with simple transformation properties can be obtained and smaller matrices will have to be solved. In the present work we will adopt the first point of view because for PbTe, which is a small gap semiconductor, quasidegeneracies occur in a large region of $\vec{k}$ space, both for the valence and conduction bands. At a symmetry point S, where some bands may have degeneracy greater than 2, and band crossing may occur between bands that transform like different irreducible representations, the situation is more critical. As far as degeneracy is concerned, two cases are possible: A single band in the region A of general points corresponds to a single band at S, or two or more bands in A will join at S, giving rise to a band with degeneracy greater than 2. The first case does not present difficulties, nor does the second case when a partner j of a band m at S corresponds to a partner i of a particular band n at all points in A near S. But this is not always true. For the Γ_8^- bands, for example, along the Δ axis the first partner of a Δ_6 band corresponds to $(b\Gamma_{8,4}^- - c\Gamma_{8,2}^-)$, where $b = (2)^{-1/2}$ and $c = (6)^{-1/2}$, while along the Σ axis the same band has to have a Σ_5 symmetry and the first partner of a Σ_5 band corresponds to $\Gamma_{8,4}^-$. In an ambiguous situation such

as the contribution coming from Γ is simply excluded without seriously affecting the integrity of the Wannier function. On the surface of the Brillouin zone, problems also arise at points $\vec{k}$ where there exist operations α in the point group such that $\alpha\vec{k} = \vec{k} + \vec{K}_i$, with $\vec{K}_i$ being a reciprocal-lattice vector. One example is the L point in the fcc lattice. Due to the special transformation properties of the wave functions, discontinuities may occur in

the $\vec{K} \cdot \vec{\pi}$ coefficients. However contributions like that can also be excluded. Points where accidental degeneracies occur can be treated in the same way. It is easy to see that the Wannier functions defined in this way form a complete orthonormal set because the Bloch function corresponding to one band contributes to one and only one Wannier function.

In the $\vec{K} \cdot \vec{\pi}$ scheme, the general term of the matrix U can be written as

$$U_{n',i';n,i}(\vec{R}_{q'},\vec{R}_q) = N_{\vec{k}}^{-1} \sum_{\vec{k}'} \sum_{\vec{k}} e^{i(\vec{k}' \cdot \vec{R}_{q'} - \vec{k} \cdot \vec{R}_q)} \sum_{m'} \sum_{j'} \sum_{m} \sum_{j} C_{n',i';m',j'}(\vec{k}')^* C_{n,i;m,j}(\vec{k}) e^{i[\Theta_n(\vec{k}) - \Theta_{n'}(\vec{k}')]}$$

$$\times \int d\vec{r}\, b_{m',j',\beta'}(\vec{k}_0,\vec{r})^* e^{i(\vec{k}-\vec{k}')\cdot\vec{r}} U(\vec{r}) b_{m,j,\beta}(\vec{k}_0,\vec{r}) . \tag{3.8}$$

In Eq. (3.8), $\vec{k}'$ and $\vec{k}$ can take general values in $\vec{k}$ space and even if a reasonable mesh of points is used, the number of matrix elements to be calculated would be enormous and the computational time involved probably prohibitive. However, if $U(\vec{r})$ is a localized perturbation we expect that simplifications can be made. In fact, if $U(\vec{r})$ is very localized near the origin, $e^{i(\vec{k}-\vec{k}')\cdot\vec{r}}$ in Eq. (3.8) can be expanded in Taylor's series near the origin and only a few terms be considered. In the case of vacancies in PbTe, as we will see later, only the first two terms need to be considered if $\vec{k}$ and $\vec{k}'$ are restricted to the first Brillouin zone. Equation (3.8) can then be written as

$$U_{n',i';n,i}(\vec{R}_{q'},\vec{R}_q) = \sum_{m'} \sum_{j'} \sum_{m} \sum_{j} \{ C_{n',i';m',j'}(\vec{R}_{q'})^* C_{n,i;m,j}(\vec{R}_q) T_{m',j';m,j}$$

$$+ [C_{n',i';m',j'}(\vec{R}_{q'})^* \vec{D}_{n,i;m,j}(\vec{R}_q) - C_{n,i;m,j}(\vec{R}_q) \vec{D}_{n',i';m',j'}(\vec{R}_{q'})] \cdot \vec{N}_{m',j';m,j} \} , \tag{3.9}$$

where

$$C_{n,i;m,j}(\vec{R}_q) = N_{\vec{k}}^{-1} \sum_{\vec{k}} C_{n,i;m,j}(\vec{k}) e^{i[\Theta_n(\vec{k}) - \vec{k}\cdot\vec{R}_q]} , \tag{3.10a}$$

$$\vec{D}_{n,i;m,j}(\vec{R}_q) = N_{\vec{k}}^{-1} \sum_{\vec{k}} \vec{k}\, C_{n,i;m,j}(\vec{k}) e^{i[\Theta_n(\vec{k}) - (\vec{k})\cdot\vec{R}_q]} , \tag{3.10b}$$

$$T_{m',j';m,j} = N_{\vec{k}} \langle b_{m',j',\beta'}(\vec{k}_0,\vec{r}) | U(\vec{r}) | b_{m,j,\beta}(\vec{k}_0,\vec{r}) \rangle , \tag{3.10c}$$

$$\vec{N}_{m',j';m,j} = iN_{\vec{k}} \langle b_{m',j',\beta'}(\vec{k}_0,\vec{r}) | \vec{r}U(\vec{r}) | b_{m,j,\beta}(\vec{k}_0,\vec{r}) \rangle . \tag{3.10d}$$

Suppose an fcc lattice and the case where the group of $\vec{k}_0$ contains inversion. The integration in $\vec{k}$ space need to be performed only over $\frac{1}{48}$ of the zone if the relations between the coefficients $C_{n,i;m,j}(\vec{k})$ and $C_{n,i;m,j}(\alpha\vec{k})$ and the phases $\Theta_n(\vec{k})$ are known. If relation (A5) is assumed, then

$$C_{n,i;m,j}(\vec{R}_q) = N_{\vec{k}}^{-1} \sum_{\vec{k}}' t(\vec{k})^{-1} \sum_{\alpha} \sum_{l} C_{n,i;m,l}(\vec{k})$$

$$\times \Gamma_\beta^{(\vec{k}_0)}(\alpha)_{j,l}\, e^{i[\Theta_n(\alpha\vec{k}) - \alpha\vec{k}\cdot\vec{R}_q]}, \tag{3.11a}$$

$$\vec{D}_{n,i;m,j}(\vec{R}_q) = N_{\vec{k}}^{-1} \sum_{\vec{k}}' t(\vec{k})^{-1} \sum_{\alpha} \sum_{l} C_{n,i;m,l}(\vec{k})$$

$$\times \Gamma_\beta^{(\vec{k}_0)}(\alpha)_{j,l}(\alpha\vec{k}) e^{i[\Theta_n(\alpha\vec{k}) - \alpha\vec{k}\cdot\vec{R}_q]} , \tag{3.11b}$$

where the primed sum in $\vec{k}$ indicates that now $\vec{k}$ is restricted to $\frac{1}{48}$ of the zone. If $\vec{k}$ is a general point, the 48 operations of the point group will give 48 different contributions in the sum on $\vec{k}$. However, if $\vec{k}$ is the Γ point, for example, the 48 operations will give 48 equal contributions and the total contribution coming from this point has to be divided by 48. This multiple counting is corrected by the weighting factor $t(\vec{k})$.

Finally, the phases $e^{i\Theta_n(\vec{k})}$ have to be chosen in order to produce reasonably localized Wannier functions. In the case of localized perturbations the Wannier functions can be considered well localized, if the matrix elements of the perturbation $U(\vec{r})$ between the Wannier functions centered at the site where the perturbation is concentrated is much larger than any other matrix elements relating Wannier functions. In order to decrease the number of possible choices for the phase factors we will assume that the phase associated with a point in the star of $\vec{k}$, where $\vec{k}$ is in $\frac{1}{48}$ of the zone, is obtained by adding a $\vec{k}$-independent constant to the phase associated with $\vec{k}$. It can be easily shown that this is a good assumption if the important $\vec{K} \cdot \vec{\pi}$ coefficients for a particular band vary in the smoothest possible

way. This is also important when interpolation is needed in order to obtain wave functions at points other than the points in the mesh. The perturbation $U(\vec{r})$ being localized at the origin we can write

$$U_{n,i;n,i}(\vec{R}_p = 0, \vec{R}_p = 0)$$

$$\simeq \sum_m \sum_{m'} \sum_j C_{n,i;m',j}(\vec{R}_p = 0)^* C_{n,i;m,j}(\vec{R}_p = 0) T_{m',m} ,$$

where we have made use of the fact that $T_{m',j';m,j} = T_{m',m} \delta_{j',j}$ and we recall that the representations corresponding to bands m' and m have to be the same. If partner i of band n corresponds to partner r of band m_s at $\vec{k}_0$ it is possible that for a large portion of the $\frac{1}{48}$ region of $\vec{k}$ space the leading $\vec{K} \cdot \vec{\pi}$ coefficient of the former band is the one corresponding to the later band. Let us emphasize this point when calculating $U_{n,i;n,i}(\vec{R}_p = 0)$. Assume that for every $\vec{k}$ in the $\frac{1}{48}$ region $C_{n,i;m_s,r}(\vec{K})$ is the leading coefficient. If band m_s transforms like the irreducible representation $\Gamma_\gamma^{(\vec{k}_0)}$, we obtain

$$U_{n,i;n,i}(\vec{R}_p = 0, \vec{R}_p = 0) \simeq A_{n,i;m_s,r} \sum_j (Q_{j,r})^* Q_{j,r} ,$$

$$(3.12)$$

where

$$A_{n,i;m_s,r} = \{N_{\vec{k}}^{-2} \sum_{\vec{k}} \sum_{\vec{k}'} [t(\vec{k}) t(\vec{k}')]^{-1} C_{n,i;m_s,r} $$
$$\times (\vec{K}')^* C_{n,i;m_s,r}(\vec{K})\} T_{m_s,m_s} ,$$

$$Q_{j,r} = \sum_j \Gamma_\gamma^{(\vec{k}_0)}(\alpha)_{j,r} e^{i\Theta_n(\alpha)} .$$

But Eq. (3.12) will be maximum if $\sum_j |Q_{j,r}|^2$ is maximum. Let $a_{j,r}$ and $b_{j,r}$ be the real and imaginary parts of $Q_{j,r}$, respectively. Then, the larger the numbers $|a_{j,r}|$ and $|b_{j,r}|$, the larger Eq. (3.12) will be. For simplicity we will assume that $e^{i\Theta_n(\alpha)} = \pm 1$. One way of obtaining a maximum value for $U_{n,i;n,i}(\vec{R}_p = 0, \vec{R}_p = 0)$ is to choose $\Theta_n(\alpha)$ such that one element, $a_{r,r}$ say, is the largest possible. But there will be some α's that do not contribute to $a_{r,r}$. Then, we choose part of the remaining $\Theta_n(\alpha)$ such that another element is the largest possible and continue in this way until all $\Theta_n(\alpha)$ have been chosen. We can now quickly choose the phase factor of an improper rotation in terms of the corresponding proper rotation, in the case where the group of $\vec{k}_0$ contains inversion. If $\Gamma_\gamma^{(\vec{k}_0)}$ has even parity, then $\Gamma_\gamma^{(\vec{k}_0)}(J\alpha) = \Gamma_\gamma^{(\vec{k}_0)}(\alpha)$, where J is the inversion operator and in this case we have to have $e^{i\Theta(J\alpha)} = e^{i\Theta(\alpha)}$. However, if $\Gamma_\gamma^{(\vec{k})}$ has odd parity, then $\Gamma_\gamma^{(\vec{k}_0)}(J\alpha) = -\Gamma_\gamma^{(\vec{k}_0)}(\alpha)$ and we should choose $e^{i\Theta(J\alpha)} = -e^{i\Theta(\alpha)}$. The Wannier functions obtained according to the above procedure are not the optimal, i.e., the most localized functions, but for PbTe, as will be discussed later, the matrix element connecting Wannier functions centered at the

origin was found to be 5–20 times larger than any other matrix element.

Recently,[26] however, it was shown that it is possible to choose the phase $\Theta_n(\vec{k})$ in order to produce optimal Wannier functions. This was accomplished by making the width or mean squared radius

$$\langle a_{n,i}(\vec{r} - \vec{R}_0) | (\vec{r} - \vec{r}_0)^2 | a_{n,i}(\vec{r} - \vec{R}_0) \rangle \text{ extremal.}$$

B. Application to PbTe

Let us apply the formalism developed in the previous sections to the case where the perturbing potential $U(\vec{r})$ is due to a neutral Pb or Te vacancy.

In the APW method the periodic potential in the crystal is assumed to be of the muffin-tin type which is obtained by placing touching spheres around the atoms in the lattice. The spherically symmetric potential (inside the spheres) is made of the Herman and Skilman's atomic potential[27] at the site under consideration plus the spherically averaged contribution of the neighboring atoms. The constant potential (outside the spheres) is chosen by linearly averaging the spherically symmetric potential in the region outside the spheres. Assume, now, that one atom, Pb say, is missing and that no lattice deformation or screening occur. The crystal potential at the sphere corresponding to this atom is only due to the contribution coming from the neighboring spheres and the perturbing potential is given by the negative of the crystal potential decreased by this contribution. In the neighboring Te spheres the spherically averaged contribution of the Pb atom is missing and it represents the perturbing potential in these spheres. The perturbing potential can be obtained in the plane-wave region by performing the same averaging used in obtaining the constant potential. It is evident that the perturbing potential constructed in such a way has the point-group symmetry and is important practically only in the cell where the vacancy is located.

First, the matrix elements of the operator $N_{\vec{k}} U(\vec{r}) \times e^{i(\vec{k}-\vec{k}')\cdot\vec{r}}$ were calculated between the nonrelativistic APW Bloch functions with ten SAPW, the cutoff in the sums on the l parameter of the spherical harmonics being $l = 10$. The convergence of the matrix elements both in the number of SAPW's and l terms was excellent. Figure 4 shows some of typical matrix elements in the case where $\Delta \vec{k} = \vec{k} - \vec{k}' = (\pi/a)(t,0,0)$, a being the lattice parameter and t varying from 0.0 to its maximum value 4.0. Two important conclusions were then deduced. First, if the representations are the same, the matrix elements are reasonably large and decreases slowly as $|\Delta \vec{k}|$ increases; second, for different representations, the matrix elements are in general small: if the representations have different parities, the matrix elements increase almost lin-
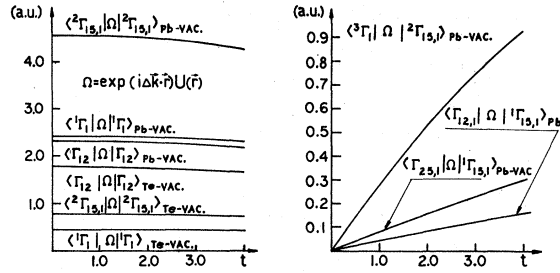
FIG. 4. Variation of some of the typical matrix elements of the operator $N_k\, e^{(i\Delta\vec{k}\cdot\vec{r})}$ between nonrelativistic single-group functions at Γ as a functions of $\Delta\vec{k}$, in the case where $\Delta\vec{k} = (\pi/a)\ (t, 0, 0)$.

early with $|\Delta\vec{k}|$, and, if the representations have the same parities, the matrix elements increase quadratically with $|\Delta\vec{k}|$. This behavior of the matrix elements provides the important key in the solution of the vacancy problem in the $\vec{K}\cdot\vec{\pi}$ scheme, because it shows that we can expand $e^{i(\vec{K}-\vec{k}')\cdot\vec{r}}$ in Taylor's series near the origin (the impurity potential is assumed to be localized near the origin), and, as a very good approximation, considers only the two first terms. This is equivalent to saying that the vacancy potential is so localized that in the Brillouin zone $e^{i\Delta\vec{k}\cdot\vec{r}}$ plays the role of a slowly varying function of $\vec{r}$. In this case we may apply the formalism deduced in the previous sections. Table V presents the values obtained for the matrix elements of $U(\vec{r})$ and $ixU(\vec{r})$ between the nonrelativistic Bloch functions at Γ. These wave

functions are such that the matrix elements are real numbers. With these matrix elements we can construct matrix T and tensor $\vec{N}$, defined by Eqs. (3.10c) and (3.10d), respectively, observing that the operator $\vec{r}U(\vec{r})$ transforms in the same way as the momentum operator under the operations of the crystal point group.

Next step in the calculations consists in obtaining for the important bands of PbTe the expressions for $C_{n,i;m,j}(\vec{R}_p)$ and $\vec{D}_{n,i;m,j}(\vec{R}_p)$ given by Eqs. (3.10a) and (3.10b). Let us consider the three valence and three conduction bands which, at Γ, corresponds to $^1\Gamma_6^-$, $^1\Gamma_8^-$, $^2\Gamma_6^-$, and $^2\Gamma_8^-$. They will be referred to as valence band numbers 3, 4, and 5 and conduction band numbers 1, 2, and 3, in the order of increasing energy. Because these bands have, over almost the entire zone, a large contribution coming from the Kohn-Luttinger functions corresponding to the above Γ_6^- and Γ_8^- bands, a reasonable choice for the phases $\Theta_n(\alpha\vec{k})$ can be made. The phases for the improper rotations are chosen such that $e^{i\Theta_n(J\alpha\vec{k})} = e^{i\Theta_n(\alpha\vec{k})}$, where J is the inversion operator. For the valence bands, the important $\vec{K}\cdot\vec{\pi}$ coefficients vary reasonably slowly over $\frac{1}{48}$ of the zone, with the exception of a region near the point in the [100] axis where band crossing and quasi-degeneracies exist. The contribution coming from $^1\Gamma_6^-$ is the largest for the lowest valence band (number 3) and although the contribution coming from the even-parity Γ bands is not small near the L point, a reasonably localized Wannier function can be obtained, if the $^1\Gamma_6^-$ contribution is optmized. This optimization consists of defining $e^{i\Theta_n(\alpha\vec{k})} = 1$

TABLE V. Matrix elements of $U(\vec{r})$ and $i \times U(\vec{r})$ between nonrelativistic bands at Γ, for Pb and Te vacancies.

		Matrix element of $U(\vec{r})$				Matrix element of $i \times U(\vec{r})$	
Band	Band	Pb vacancy (a.u.)	Te vacancy (a.u.)	Band	Band	Pb vacancy (a.u.)	Te vacancy (a.u.)
$^1\Gamma_1$	$^1\Gamma_1$	2.397	0.468	$^1\Gamma_1$	$^1\Gamma_{15,1}$	0.007	-0.824
$^1\Gamma_1$	$^2\Gamma_1$	-1.474	1.065	$^1\Gamma_1$	$^2\Gamma_{15,1}$	0.013	0.345
$^1\Gamma_1$	$^3\Gamma_1$	-1.239	-1.054	$^2\Gamma_1$	$^1\Gamma_{15,1}$	-0.069	0.103
$^2\Gamma_1$	$^2\Gamma_1$	0.921	2.466	$^2\Gamma_1$	$^2\Gamma_{15,1}$	-0.162	-0.039
$^2\Gamma_1$	$^3\Gamma_1$	0.751	-2.364	$^3\Gamma_1$	$^1\Gamma_{15,1}$	-0.113	0.370
$^3\Gamma_1$	$^3\Gamma_1$	0.648	2.413	$^3\Gamma_1$	$^2\Gamma_{15,1}$	-0.274	-0.152
$^1\Gamma_{15,1}$	$^1\Gamma_{15,1}$	0.752	4.085	$\Gamma_{12,1}$	$^1\Gamma_{15,1}$	-0.084	0.121
$^1\Gamma_{15,1}$	$^2\Gamma_{15,1}$	1.768	-1.686	$\Gamma_{12,1}$	$^2\Gamma_{15,1}$	-0.162	-0.029
$^2\Gamma_{15,1}$	$^2\Gamma_{15,1}$	4.534	0.800	$\Gamma'_{25,1}$	Γ'_2	-0.005	-0.019
$\Gamma_{12,1}$	$\Gamma_{12,1}$	2.305	1.774	$\Gamma'_{25,1}$	$^1\Gamma_{15,1}$	0.047	-0.124
Γ'_2	Γ'_2	0.160	0.143	$\Gamma'_{25,1}$	$^2\Gamma_{15,1}$	0.123	0.048
$\Gamma'_{25,1}$	$\Gamma'_{25,1}$	1.575	1.190				

for all proper rotations. Although throughout a large part of the $\frac{1}{48}$ region of the Brillouin zone the valence band numbers 4 and 5 consist primarily of the Kohn-Luttinger functions coming from the first and third partners of $^1\Gamma_8^-$, reasonably large contributions also come from the other partners of $^1\Gamma_8^-$, from the Γ_6^- bands and from $^2\Gamma_8^-$, besides the contribution from the even-parity Γ bands. For both valence bands, the most localized Wannier functions were obtained not when the contribution coming from the first and third partners of $^1\Gamma_8^-$ were optimized, but when all partners of $^1\Gamma_8^-$ were optimized. This corresponds to the choice $e^{i\Theta(\alpha)} = \pm 1$, according to $\chi_8^-(\alpha) \gtrless 0$, where $\chi_8^-(\alpha)$ denotes the character of the matrix representing α in the Γ_8^--irreducible representation. But, there are some α for which $\chi_8^-(\alpha) = 0$ and the corresponding phase factors remain undefined. The optimization of Γ_6^-, which corresponds to the choice $e^{i\Theta(\alpha)} = 1$ for all α was the one that produced the best Wannier functions. The conduction bands are also represented by slowly varying $\vec{K} \cdot \vec{\pi}$ coefficients, except in regions near the points where accidental and quasidegeneracies exist. Although the lowest conduction band (number 1) also has a large contribution coming from the Γ_8^- bands, the optimization of the Γ_6^- bands proved to give better results. The other two bands behaved in the same way as the two upper valence bands, as far as the choice of the phase factors is concerned. Besides the three above-mentioned valence bands, PbTe also has two other valence bands which are important in the vacancy problem. These bands will be called valence band numbers 1 and 2, and at Γ they correspond to $^3\Gamma_6^+$ and $^1\Gamma_6^+$, respectively. Valence band 1 has an averaged contribution of 0.897 coming from the Kohn-Luttinger function corresponding to $^3\Gamma_6^+$ and valence band number 2 has an averaged contribution of 0.731 coming from $^1\Gamma_6^+$. This means that very localized Wannier functions can be constructed for these bands if $e^{i\Theta(\alpha\vec{k})} = 1$ for all α. In the determination of the vacancy energy levels, the conduction band that at Γ corresponds to $^2\Gamma_6^+$ had to be included in the calculations, because it has an averaged contribution of 0.627 coming from $^2\Gamma_6^+$ and the matrix elements of the impurity potential connecting $^2\Gamma_6^+$ and $^3\Gamma_6^+$ and $^1\Gamma_6^+$ are very large.

Once the coefficients $C_{n,i;m,j}(\vec{R}_q)$ and $\vec{D}_{n,i;m,j}(\vec{R}_q)$ are known, the matrix elements of $U(\vec{r})$ between Wannier functions can be obtained. Those matrix elements were calculated for the five valence bands and four conduction bands and for the site at the origin and 12 nearest neighbors of the type $\vec{R}_q = (\frac{1}{2}a)(1, 1, 0)$. We have found that, for all bands, the matrix elements connecting Wannier functions centered at the origin were 5 to 20 times larger than any other matrix element.

On the other hand, matrix G is diagonal in both the band and partner indices. Then

$$G_{n,i;n,i}(\Delta\vec{R}_q, E)$$

$$= N_{\vec{k}}^{-1} \sum_{\vec{k}}' \sum_\alpha 2[E - E_n(\vec{k})]^{-1} \cos(\alpha\vec{k} \cdot \Delta\vec{R}_q),$$

where $\Delta\vec{R}_q = \vec{R}_q - \vec{R}_{q'}$, the sum on $\vec{k}$ is performed in $\frac{1}{48}$ of the zone and the sum on α includes only the 24 proper rotations of the crystal point group. We can observe that $G_{n,i;n,i}(-\Delta\vec{R}_q, E) = G_{n,i;n,i}(\Delta\vec{R}_q, E)$. Due to the fact that, for values of E near the top or bottom of the energy band, the G matrix depends strongly on the details of the band near these maxima, the number and distribution of points in the energy mesh are very important. We have calculated the elements of G for some values of E near and far from the extremum of the bands using both the regular and Conroy's[28] integration methods. For all bands very good convergence was obtained for a Conroy's mesh of 1000 points in $\frac{1}{48}$ of the zone. As continuous energy bands have been defined in $\vec{k}$ space, $G_{n,i;n,i}(\Delta\vec{R}_q, E)$ properly approaches zero for large values of E.

As the vacancy potential has the crystal point-group symmetry, the wave functions corresponding to the bound states will have to transform like the irreducible representations of the crystal point group. Thus, instead of diagonalizing the total matrix $[G_{NN}^{-1} - U_{NN}]$, we factor it in block form, each block containing only states with wave functions transforming as the same irreducible representations. This factorization can be accomplished using projection operators, if the transformation properties of the Wannier functions are known. Although providing a proper G matrix, our definition of Wannier functions do not produce functions with simple transformation properties. Because of that, as proved in Appendix B, we can only factor the total matrix U or G into two smaller matrices, one for the even-parity representations and other for the odd-parity representations. These two blocks cannot be easily factored into smaller blocks containing only one irreducible representation, but each block is totally diagonalized. In the following discussion we will call the energy levels obtained from the even-parity and odd-parity blocks, symmetric and antisymmetric levels, respectively.

The symmetric and antisymmetric energy levels obtained in the single-band approximation for the five valence bands are shown in Table VI. There we present the results for one site and 13 sites. In the first case only one symmetric state is produced per band, while in the second case, seven symmetric and six antisymmetric levels exist for each band. For vacancy potentials in PbTe the perturbation is not strong enough to pull antisymmetric states out of the bands, and only symmetric bound states may occur. For a Pb vacancy one

TABLE VI. Symmetric and antisymmetric states obtained in the single-band approximation for the valence bands of PbTe. The zero of energy is taken at the top of the corresponding band.

Band	Vacancy	Number of sites	Symmetric In the band	Symmetric Bound states $(10^{-3}\mathrm{Ry})$	Anti-symmetric In the band
Valence 1	Pb	1	0	52.03	0
		13	6	94.22	6
Valence 2	Pb	1	0	631.18	0
		13	6	758.37	6
Valence 3	Pb	1	1	$\cdots$	0
		13	7	$\cdots$	6
Valence 4	Pb	1	1	$\cdots$	0
		13	7	$\cdots$	6
Valence 5	Pb	1	1	$\cdots$	0
		13	7	$\cdots$	6
Valence 1	Te	1	0	1122.32	0
		13	6	1278.27	6
Valence 2	Te	1	0	43.22	0
		13	6	75.13	6
Valence 3	Te	1	0	123.81	0
		13	6	137.85	6
Valence 4	Te	1	0	38.75	0
		13	6	57.70	6
Valence 5	Te	1	0	16.43	0
		13	5	39.01	6
				26.52	

symmetric bound state is produced both for valence band 1 and 2. The effect of considering more sites is to increase the energy of these states. The perturbation, however, is not strong enough to produce symmetric bound states for valence bands 3–5. A different picture is produced when a Te vacancy is present in PbTe. Now, besides valence bands 1 and 2, symmetric bound states are also pulled out of the valence bands 3–5. All these bands, except valence band number 5, present only one symmetric bound state both for one and 13 sites. For valence band 5, however, one state exists when one site is considered, but another one appears when 13 sites are taken into account. Then, in the single-band approximation and 13 sites, one bound state appears above the bottom of the lowest conduction band for a Pb vacancy and, for a Te vacancy, the number of bound states is equal to three.

Finally, all the five valence bands and four conduction bands were considered together. For 13 sites the resulting symmetric and antisymmetric matrices have dimensions of 63 and 54, respectively. But due to the fact that valence band 1 and 2 and conduction band 4 have a large contribution coming from the Γ_6^+ levels and the other bands have a large contribution coming from the Γ_6^- and Γ_8^- levels, these two groups can be considered separately. We are allowed to make this separation not only because the matrix elements $\langle \Gamma_6^+ | U(\vec{r}) | \Gamma_6^-$ or $\Gamma_8^-\rangle$ are smaller than $\langle \Gamma_6^+ | U(\vec{r}) | \Gamma_6^+\rangle$ or $\langle \Gamma_6^-$ or $\Gamma_8^- | U(\vec{r})$ $\times | \Gamma_6^-$ or $\Gamma_8^-\rangle$ but also because they enter tensor $\bar{\bar{N}}$ which gives a second-order contribution to the matrix element of U between Wannier functions. When all bands are considered we can only look for bound states for values of E outside the bands. This means that in the first group we look for solutions with energy between the top of valence band 2 and bottom of conduction band 4. In the second group, only energies in the gap can be considered. But, by investigating the dependence of the eigenvalues of the matrix $[G_{NN}^{-1} - U_{NN}]$ on the energy E we can determine the number of states lying below and above a given energy E. For the first group only one symmetric bound state was found at $-0.4329\,\mathrm{Ry}$, for a Pb vacancy, and at $-0.2386\,\mathrm{Ry}$, for a Te vacancy. In both cases, the effect of the interaction between the bands was to decrease the energy of the bound state obtained in the single-band approximation, between the top of the valence band 2 and bottom of conduction band 4. This level, however, still lies well above the gap. For the second group, no bound state was found in the gap either for a Pb or Te vacancy. Comparing with the unperturbed case, no extra state appears or disappears above and below the gap, in the case of a Pb vacancy, but, for a Te vacancy, three extra states were found above the gap and, consequently, three states disappear below it. If the results of the two groups are considered together, we conclude that both for a Pb and a Te vacancy no bound states are produced in the gap. For a Te vacancy three states disappear below the energy gap and appear above it, while for a Pb vacancy, only one state disappears below the gap and appears above it.

A Pb atom (configuration $6s^2 6p^2$) contributes four valence electrons while a Te atom (configuration $5s^2 5p^4$) contributes six. If a Pb vacancy is present in the crystal, then the perturbed crystal has four fewer electrons than the perfect crystal. But as only one state (which can accomodate two electrons) has moved from the valence to the conduction bands, there is still an empty state in the valence bands. Therefore two holes are available in the valence band and we have a p-type semiconductor, in which the carriers cannot be frozen out. On the other hand, if a Te vacancy exists, the perturbed crystal has six fewer electrons than the unperturbed crystal. But as four states have moved from the valence to the conduction bands, then there is one state filled in the conduction band, i.e., two electrons are available there. An n-type semiconductor is produced and again the carriers cannot be frozen out. These results are shown in Fig. 5.

It is interesting to note here that the number of states pulled out of the bands depends on both the strength of the perturbation and on the shape of the
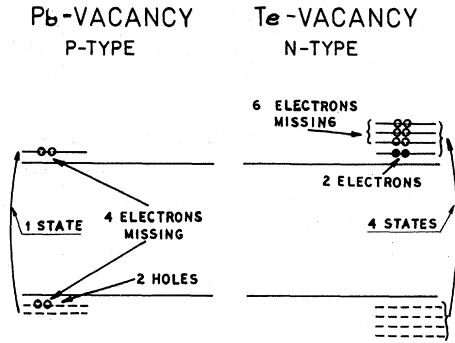
FIG. 5. Schematic representation of the effect of a Pb and a Te vacancy.

energy bands. The first dependence is present in the U matrix, while the second is present in the G matrix. Because we have calculated the G matrix using a Conroy's mesh of 1000 points, a point corresponding to the top of the band probably does not occur in this mesh. Now, if we allow the energy to have values between the top of the band and the highest energy in the mesh, other bound states may occur, when more than one site is considered. This indeed happens in PbTe. In order to decide whether these levels are bound states or not it is necessary to calculate the G matrix for energies very near the top of the band using a very large mesh of points. However, we believe that in PbTe these states are in the band because the comparison of the present mesh of 1000 points with the regular meshes of 152 and 916 points, which do include the top of the band, shows that the value obtained with Conroy's mesh is the convergent value. Even if some of these states were bound states, they are so close to the band that screening will be very important. But as the dielectric constant of PbTe is high the effective perturbative potential will be much smaller than the potential we have used in the present calculation and, as a consequence, these states will be moved further towards the top of the band.

ACKNOWLEDGMENTS

APPENDIX A

Let us determine the properties of the Bloch functions obtained in the $\vec{K} \cdot \vec{\pi}$ scheme in the case where the group of $\vec{k}_0$ is the point group of the crystal. If $\{\alpha | \vec{a}\}$ is a general operation of the space group we have

$$\{\alpha | \vec{a}\} b_{n,i,\gamma}(\vec{k}, \vec{r}) = \sum_m \sum_j C_{n,i;m,j}(\vec{K}) e^{i\alpha \vec{K} \cdot (\vec{r}+\vec{a})}$$

$$\times \sum_l \Gamma_\beta^{(\vec{k}_0)}(\alpha)_{l,j} b_{m,l,\beta}(\vec{k}_0, \vec{r}), \quad \text{(A1)}$$

$$b_{n,i,\gamma}(\alpha \vec{k}, \vec{r}) = \sum_m \sum_j C_{n,i;m,j}(\alpha \vec{K}) e^{i\alpha \vec{K} \cdot \vec{r}} b_{m,j,\beta}(\vec{k}_0, \vec{r}),$$

$$\text{(A2)}$$

where we have made use of Eq. (2.4) and the fact that $\alpha \vec{k}_0 = \vec{k}_0$. In order to relate Eqs. (A1) and (A2) it is necessary to obtain the relation between $C_{n,i;m,j}(\vec{K})$ and $C_{n,i;m,j}(\alpha \vec{K})$.

The general term in the $\vec{K} \cdot \vec{\pi}$ secular matrix at $\alpha \vec{k}$ is given by

$$[E_{m'}(\vec{k}_0) + (2m)^{-1}(\hbar \vec{K})^2 - (8m^3 c^2)^{-1}(\hbar \vec{K})^4 - E_n(\alpha \vec{k})] \delta_{n,m'}$$

$$\times \delta_{i,j} + m^{-1} \hbar \alpha \vec{K} \cdot \langle b_{n,i,\beta}(\vec{k}_0, \vec{r}) | \vec{\pi} | b_{m',j,\beta'}(\vec{k}_0, \vec{r}) \rangle.$$

$$\text{(A3)}$$

As for practical purposes $\vec{\pi}$ can be replaced by only $\vec{p}$,

$$\langle b_{n,i,\beta}(\vec{k}_0, \vec{r}) | \vec{\pi} | b_{m',j,\beta'}(\vec{k}_0, \vec{r}) \rangle$$

$$= \langle \alpha b_{n,i,\beta}(\vec{k}_0, \vec{r}) | (\alpha^{-1} \vec{\pi}) | \alpha b_{m',j,\beta'}(\vec{k}_0, \vec{r}) \rangle$$

and

$$\alpha^{-1} \langle b_{n,i,\beta}(\vec{k}_0, \vec{r}) | \vec{\pi} | b_{m',j,\beta'}(\vec{k}_0, \vec{r}) \rangle$$

$$= \langle \alpha^{-1} b_{n,i,\beta}(\vec{k}_0, \vec{r}) | \vec{\pi} | \alpha^{-1} b_{m',j,\beta'}(\vec{k}_0, \vec{r}) \rangle,$$

and the term (A3) becomes

$$[E_{m'}(\vec{k}_0) + (2m)^{-1}(\hbar \vec{K})^2 - (8m^3 c^2)^{-1}(\hbar \vec{K})^4 - E_n(\alpha \vec{k})] \delta_{n,m'}$$

$$\times \delta_{i,j} + m^{-1} \hbar \vec{K} \cdot \langle \alpha^{-1} b_{n,i,\beta}(\vec{k}_0, \vec{r}) | \vec{\pi} | \alpha^{-1} b_{m',j,\beta'}(\vec{k}_0, \vec{r}) \rangle.$$

$$\text{(A4)}$$

But (A4) is also the general term of the $\vec{K} \cdot \vec{\pi}$ secular equation at $\vec{k}$, the basis being $e^{i\vec{K} \cdot \vec{r}} \alpha^{-1} b_{m,l,\beta}(\vec{k}_0, \vec{r})$, i.e.,

$$b_{n,i,\gamma}(\vec{k}, \vec{r}) = \sum_m \sum_l C_{n,i;m,l}(\alpha \vec{K}) (e^{i\vec{K} \cdot \vec{r}}) \alpha^{-1} b_{m,l,\beta}(\vec{k}_0, \vec{r})$$

As

$$\alpha^{-1} b_{m,l,\beta}(\vec{k}_0, \vec{r}) = \sum_j \Gamma_\beta^{(\vec{k}_0)}(\alpha^{-1})_{j,l} b_{m,j,\beta}(\vec{k}_0, \vec{r})$$

we conclude that

$$C_{n,i;m,j}(\alpha \vec{K}) = \sum_l C_{n,i;m,l}(\vec{K}) \Gamma_\beta^{(\vec{k}_0)}(\alpha)_{j,l}, \quad \text{(A5)}$$

where we have made use of the unitary nature of $\Gamma_\beta^{(\vec{k}_0)}(\alpha^{-1})$. Comparison between (A5) and (A1) gives

$$\{\alpha | \vec{a}\} b_{n,i,\gamma}(\vec{k}, \vec{r}) = (e^{i\alpha \vec{k} \cdot \vec{a}}) b_{n,i,\gamma}(\alpha \vec{k}, \vec{r}). \quad \text{(A6)}$$

APPENDIX B

Let us determine the transformation properties of the Wannier functions for an fcc lattice. If β is an operation of the crystal point group, then

$$\beta a_{n,i}(\vec{r} - \vec{R}_q) = \sum_m \sum_p (N_{\vec{k}})^{-1} \sum_{\vec{k}}' [t(\vec{k})]^{-1} \sum_\alpha \sum_l C_{n,i;m,l}(\vec{K})$$

$$\times \; \Gamma_\gamma^{(\vec{k}_0)}(\beta\alpha)_{p,l} \; e^{i[\Theta_n(\alpha\vec{k}) - \alpha\vec{k}\cdot\vec{R}_q]} b_{m,p,\gamma}(\vec{k}_0, \vec{r}) \; . \quad (B1)$$

If spin is not present, $\delta = \beta\alpha$ is one of the 48 operations contained in the sum on α. Then

$$\beta a_{n,1}(\vec{r} - \vec{R}_q) = \sum_m \sum_p (N_{\vec{k}})^{-1} \sum_{\vec{k}}' [t(\vec{k})]^{-1} \sum_\delta \sum_l C_{n,1;m,l}(\vec{K})$$

$$\times \; \Gamma_\gamma^{(\vec{k}_0)}(\delta)_{p,l} \; e^{i[\Theta_n(\beta^{-1}\alpha\vec{k}) - \delta\vec{k}\cdot\beta\vec{R}_q]} b_{m,p,l}(\vec{k}_0, \vec{r}) \; , \quad (B2)$$

and if for a given $\vec{k}$ the same phase factor corresponds to all operations δ, we obtain

$$\beta a_{n,1}(\vec{r} - \vec{R}_q) = a_{n,1}(\vec{r} - \beta\vec{R}_q) \; . \quad (B3)$$

In the present calculation we are dealing with double-group representations and $\delta = \beta\alpha$ is not necessarily one of the 48 operations contained in the sum on α. Besides that, in order to produce local-ized Wannier functions the above choice of the phase factors is not always possible. For the inversion operator J, however, $\delta = \beta\alpha$ is always one of the 48 operations and $Ja_{n,i}(\vec{r} - \vec{R}_q) = \pm a_{n,i}(\vec{r} + \vec{R}_q)$ if we choose $e^{i\Theta_n(J\delta\vec{k})} = \pm e^{i\Theta_n(\delta\vec{k})}$, which is consistent with the present choices for the phase factors. Then

$$\langle a_{m,i}(\vec{r} - \vec{R}_p) | U(\vec{r}) | a_{n,i}(\vec{r} - \vec{R}_q) \rangle$$

$$= \pm \langle a_{m,i}(\vec{r} + \vec{R}_p) | U(\vec{r}) | a_{n,i}(\vec{r} + \vec{R}_q) \rangle \; ,$$

depending upon whether band m and n have the same or different choices for $e^{i\Theta_n(J\delta\vec{k})}$.

We may construct for each band the symmetric and antisymmetric linear combinations

$$\Psi_{n,i}^s(\vec{r}, \vec{R}_p) = (2)^{-1/2} [a_{n,i}(\vec{r} - \vec{R}_p) + a_{n,i}(\vec{r} + \vec{R}_p)] \; ,$$

$$\Psi_{n,i}^{as}(\vec{r}, \vec{R}_p) = (2)^{-1/2} [a_{n,i}(\vec{r} - \vec{R}_p) - a_{n,i}(\vec{r} + \vec{R}_p)] \; ,$$

and obtain

$$\langle \Psi_{n,i}^s(\vec{r}, \vec{R}_p) | U(\vec{r}) | \Psi_{m,i}^{as}(\vec{r} - \vec{R}_q) \rangle = 0 \; .$$

If $\vec{R}_p = 0$, we have only the symmetric function

$$\Psi_{n,i}^s(\vec{r}, \vec{0}) = a_{n,i}(\vec{r} - \vec{0}) .$$

[†]Based on the doctoral dissertation for the degree of Doctor of Philosophy in Electrical Engineering at M.I.T. Research supported by the U. S. Army Research (Durham).

[*]Present address: Instituto de Física, Universidade Estadual de Campinas, CP 1170, Campinas, S.P., Brasil.

[1]N. J. Parada and G. W. Pratt, Jr., Phys. Rev. Letters **22**, 180 (1969).

[2]W. Pearson, *Handbook of Lattice Spacings and Structure of Metal and Alloys* (Pergamon, New York, 1958).

[3]W. W. Scanton, J. Phys. Chem. Solids **8**, 423 (1959).

[4]V. Prakash, Ph.D. thesis, Harvard University, 1967 (unpublished).

[5]K. F. Cuff, M. R. Ellett, and C. D. Kuglin, in *Proceedings of the International Conference on Physics of Semiconductors*, 1962 (The Institute of Physics and Physical Society, London, 1962), p. 316; J. Appl. Phys. Suppl. **32**, 2179 (1961).

[6]M. B. Seltzer and J. B. Wagner, Jr., J. Chem. Phys. **36**, 130 (1962).

[7]H. Gobrecht and A. Richter, J. Phys. Chem. Solids **26**, 1889 (1965).

[8]M. B. Seltzer and J. B. Wagner, Jr., J. Phys. Chem. Solids **24**, 1525 (1963).

[9]A. J. Crocker, J. Phys. Chem. Solids **28**, 1903 (1967).

[10]J. Callaway and A. J. Hughes, Phys. Rev. **156**, 860 (1967); **164**, 1043 (1967).

[11]G. F. Koster and J. C. Slater, Phys. Rev. **95**, 1167 (1954); **96**, 1208 (1954).

[12]See, for example, J. Sokoloff, Phys. Rev. **161**, 540 (1967).

[13]G. F. Koster, Phys. Rev. **95**, 1436 (1954); J. Callaway, J. Math. Phys. **5**, 783 (1964).

[14]J. B. Conklin, Jr., Ph.D. thesis, Massachusetts Institute of Technology, 1964 (unpublished); J. B. Conklin, Jr., L. E. Johnson, and G. W. Pratt, Jr., Phys. Rev. **137**, A1282 (1965).

[15]P. J. Lin and L. Kleinman, Phys. Rev. **142**, 478 (1966).

[16]G. W. Pratt, Jr., and L. G. Ferreira, in *Proceedings of the International Conference on Physics of Semiconductors, Paris*, 1964 (Academic, New York, 1965), p. 69.

[17]L. G. Ferreira, Phys. Rev. **137**, A1601 (1965).

[18]H. Cardona and F. H. Pollack, Phys. Rev. **142**, 530 (1966).

[19]F. Herman, in Ref. 16, p. 3.

[20]D. Brust, Phys. Rev. **134**, A1337 (1964).

[21]L. L. Foldy and S. A. Wouthuysen, Phys. Rev. **78**, 29 (1950).

[22]See, for example, G.F. Koster, in *Solid State Physics*, edited by F. Seitz and D. Turnball (Academic, New York, 1957).

[23]J. Callaway, Phys. Letters **264**, 114 (1968).

[24]D. D. Buss and N. J. Parada, Phys. Rev. B **1**, 2692 (1970).

[25]M. Cardona and D. L. Greenaway, Phys. Rev. **133**, A1685 (1964).

[26]L. G. Ferreira and N. J. Parada, Phys. Rev. B **2**, 1614 (1970).

[27]F. Herman and S. Skillman, *Atomic Structure Calculations* (Prentice-Hall, Englewood Cliffs, N. J., 1963).

[28]H. Conroy, J. Chem. Phys. **47**, 5307 (1967).